CHEMISTRY
A EUROPEAN JOURNAL

DOI: 10.1002/chem.201001364

Effects of Alkyl Chain Length on Properties of 1-Alkyl-3-methylimidazolium Fluorohydrogenate Ionic Liquid Crystals

Fei Xu, Kazuhiko Matsumoto,* and Rika Hagiwara[a]

Abstract: A series of 1-alkyl-3-methylimidazolium fluorohydrogenate salts (C_xMIm$(FH)_2$F, $x=8$, 10, 12, 14, 16, and 18) have been characterized by thermal analysis, polarized optical microscopy, IR spectroscopy, X-ray diffraction, and anisotropic ionic conductivity measurements. Liquid crystalline mesophases with a smectic A interdigitated bilayer structure are observed from C_{10} to C_{18}, showing a fan-like or focal conic texture. The temperature range of the mesophase increases with the increase in the alkyl chain length (from 10.1 °C for C_{10}MIm$(FH)_2$F to 123.1 °C for C_{18}MIm$(FH)_2$F). The distance between the two layers in the smectic structure gradually increases with increasing alkyl chain length and decreases with increasing temperature. Conductivity parallel to the smectic layers is around 10 mS cm^{-1} regardless of the alkyl chain length, whereas that perpendicular to the smectic layers decreases with increasing alkyl chain length because of the thicker insulating sheet with the longer alkyl chain.

Keywords: conducting materials · ionic liquids · liquid crystals · mesophases

Introduction

Ionic liquids are widely studied as reaction media and electrolytes because of their unique properties, such as wide liquid temperature range, negligible vapor pressure, and nonflammability.[1] In particular, imidazolium-based ionic liquids attract considerable attention since they give low melting points with high chemical and electrochemical stability. Ionic liquid crystals (ILCs) can be considered as substances that possess the properties of both ionic liquids and liquid crystals, being composed of ionic species and exhibiting a liquid crystalline mesophase in a certain temperature range.[2] Because of the widespread use of imidazolium-based ionic liquids, imidazolium-based ILCs are frequently studied.[3] For example, 1-alkyl-3-methylimidazolium cations with long alkyl chains were combined with various anions, such as chloride (Cl),[4] bromide (Br),[5] tetrachlorometallate (MCl_4, M = Co and Ni),[4] hexafluorophosphate (PF_6),[6] tetrafluoroborate (BF_4),[7] and trifluoromethanesulfonate (OSO_2CF_3).[5] The temperature range of the mesophase observed for these salts rapidly increases with increasing alkyl chain length, although the alkyl chain length at which liquid crystalline mesophases appear depends on the anionic species.

Ionic liquid crystals are interesting candidates to design anisotropic ion-conductive materials since they have an anisotropic structural organization composed of only ionic species.[2] Depending on the types of liquid crystalline mesophases, 1D[8–9] or 2D[10–11] ion conduction can be achieved by use of fan-shaped or smectic ILCs, respectively, where the high anisotropy in ionic conductivity can be obtained in both the cases. However, the conductivity of these anisotropic ion-conductive materials is not sufficient for practical applications (10^0–10^1 mS cm^{-1}) so far. Although one type of columnar liquid-crystalline assembly formed through noncovalent intermolecular interactions was reported to exhibit ionic conductivities between 1 and 10 mS cm^{-1} at ambient temperature,[9] further improvement in ionic conductivity at room temperature is still in great demand.

Since the first report of 1-ethyl-3-methylimidazolium fluorohydrogenate in 1999,[12] a series of fluorohydrogenate ionic liquids with alkylimidazolium, alkylpyridinium, alkylpyrrolidinium, and alkylpiperidinium cations has been prepared and characterized.[13–16] Fluorohydrogenate ionic liquids contain the $(FH)_nF^-$ anions exhibiting high ionic conductivities (100 mS cm^{-1} for 1-ethyl-3-methylimidazolium fluorohydrogenate, EMIm$(FH)_{2.3}$F).[14] Such a high conductivity of fluorohydrogenate ionic liquids makes them attrac-

[a] F. Xu, Prof. K. Matsumoto, Prof. R. Hagiwara
Graduate School of Energy Science
Kyoto University, Yoshida, Sakyo-ku
Kyoto 606-8501 (Japan)
Fax: (+81) 75-753-5906
E-mail: k.matsumoto@ky7.ecs.kyoto-u.ac.jp

Supporting information for this article is available on the WWW under http://dx.doi.org/10.1002/chem.201001364.

tive materials as electrolytes in various electrochemical devices, such as electrochemical capacitors[17] and fuel cells.[18]

Herein, a series of 1-alkyl-3-methylimidazolium fluorohydrogenate salts ($C_xMIm(FH)_2F$, $x=8$, 10, 12, 14, 16, and 18) were characterized by several techniques. Incorporation of $(FH)_nF^-$ into the ionic liquid crystals can lead to high anisotropic ionic conductivity, since fluorohydrogenate ionic liquids exhibit high conductivity. Such materials are potential electrolytes in electrochemical systems in which the diffusion of $(FH)_nF^-$ is involved with electrode reactions including fluorohydrognate fuel cells[18] and electrochemical fluorination.[19] The imidazolium cations with a normal alkyl chain were chosen because the simple structure with high chemical and electrochemical stability is preferable to see the effects of alkyl chain length on liquid crystalline behavior.[1] Physicochemical properties and structures of the obtained fluorohydrogenate salts were studied by IR spectroscopy, differential scanning calorimetry (DSC), polarized optical microscopy (POM), and X-ray diffraction (XRD). Anisotropic conductivity parallel and perpendicular to smectic layers was measured for the liquid crystalline mesophase.

Results and Discussion

Synthesis: The fluorohydrogenate salts in the present study were prepared by the reaction of the corresponding chloride and a large excess of anhydrous HF.[12–15,17] When the alkyl chain is short, the vacuum-stable HF composition in fluorohydrogenate ionic liquids is 2.3 (namely, $Cat^+(FH)_{2.3}F$ (Cat^+ = cation)) at room temperature regardless of the cationic structure (imidazolium, pyridinium, pyrrolidinium, and piperidinium),[12–15,17] although this is not the case when the resulting salt is solid at room temperature. At this composition, the two anions $(FH)_2F^-$ and $(FH)_3F^-$ are mixed in the ratio of 7 to 3 to satisfy the composition. The present study reveals that extension of the alkyl chain seems to break this rule and the resulting vacuum-stable HF composition n for $C_xMIm(FH)_nF$ ($x=8$, 10, 12, 14, 16, and 18) at room temperature ranges from 2.0 to 2.3, which probably arises from the stronger hydrophobic interactions between the chains by the introduction of a long alkyl chain. To see the effects of the alkyl chain length on the $C_xMIm(FH)_nF$ salts, the n value was adjusted to 2.0 by either removing HF at elevated temperatures or mixing two fluorohydrogenate salts with n values less than and greater than 2.0 (see Scheme 1 for the structures of C_xMIm^+ and $(FH)_2F^-$). All of the resulting salts do not have a detectable HF dissociation pressure up to temperatures around 45 °C. The $(FH)_nF^-$ anions can be best identified by IR spectroscopy.[20] The $(FH)_2F^-$ anion

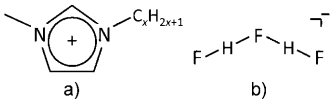

Scheme 1. Structures of a) C_xMIm^+ and b) $(FH)_2F^-$.

with a bent molecular shape (C_{2v}) was confirmed by broad absorption bands at approximately 450, 1050, 1800, 2000, and 2350 cm^{-1} in the IR spectra of all the $C_xMIm(FH)_2F$ salts (Figure S1, Supporting Information).[21] The $C_xMIm(FH)_2F$ salts ($x=8$, 10, and 12) are viscous liquids at room temperature and the viscosity appears to increase with an increase in x. The $C_xMIm(FH)_2F$ ($x=14$, 16, and 18) salts are wax-like solids at room temperature. Hygroscopicity and solubility in water of these fluorohydrogenate salts decrease as the alkyl chain becomes longer.

Thermal properties: Thermogravimetric (TG) analysis revealed that $C_xMIm(FH)_2F$ slowly loses HF at elevated temperatures and decomposes around 230 °C regardless of the alkyl chain length (Figure S2, Supporting Information). This behavior is similar to the other fluorohydrogenate salts with short alkyl chains.[13] The DSC curves of $C_xMIm(FH)_2F$ are shown in Figure 1 and the DSC data obtained (transition temperatures, ΔH, and ΔS) are summarized in Table 1. Only the heating process is shown for each sample, since the fluorohydrogenate salts slowly liberate HF at temperatures above 45 °C,[20] leading to a decrease in the n value, and precise measurement on the cooling process was difficult. For $C_xMIm(FH)_2F$ ($x=12$, 14, 16, and 18), two endothermic peaks are observed in the thermograms. The endothermic

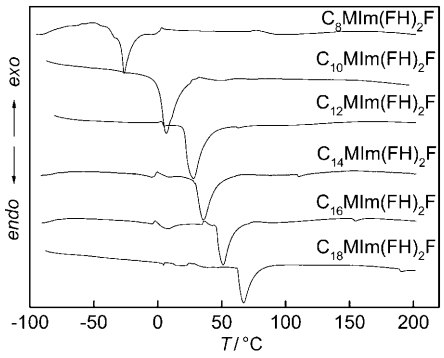

Figure 1. Differential scanning calorimetric curves (heating process) for $C_xMIm(FH)_2F$ ($x=8$, 10, 12, 14, 16, and 18).

Table 1. Summary of the DSC analysis for $C_xMIm(FH)_2F$ ($x=8$, 10, 12, 14, 16, and 18).

x	Transition[a]	T [°C]	ΔH [kJ mol^{-1}]	ΔS [J mol^{-1} K^{-1}]
8	cryst–iso	−28.1	12.4	49.0
10	cryst–SmA_2	−0.1	18.0	64.3
	SmA_2–iso	10.0[b]	_[b]	_[b]
12	cryst–SmA_2	20.2	19.9	66.1
	SmA_2–iso	61.5	0.11	0.33
14	cryst–SmA_2	29.0	20.1	65.1
	SmA_2–iso	109.2	0.31	0.81
16	cryst–SmA_2	45.5	21.7	66.9
	SmA_2-iso	152.6	0.43	1.01
18	cryst-SmA_2	62.2	27.7	81.4
	SmA_2–iso	188.8	0.43	0.93

[a] The symbols cryst, iso, and SmA_2 denote crytstal, isotropic liquid, and smectic A_2 liquid crystal. [b] This transition temperature was determined by XRD and ΔH and ΔS could not be obtained because the DSC peak overlapped the peak of the cryst–SmA_2 transition.

peaks at the lower temperature (with a large ΔH) and the higher temperature (with a small ΔH) correspond to the melting point (from crystal to liquid crystal) and the clearing temperature (from liquid crystal to isotropic liquid), respectively. The relatively large ΔH (and thus ΔS) on melting indicates a considerable structural change, namely, the breakup of a three-dimensionally ordered crystal lattice. The small ΔH (and thus ΔS) at the clearing temperature is mainly caused by the breakup of van der Waals interactions between the alkyl chains, which is reflected in the increase of ΔH (and thus ΔS) at clearing temperatures with the increase in x. Similar phenomena were also observed for ILCs, 1-alkyl-3-methylimidazolium chloride, bromide, hexafluorophosphate, and tetrafluoroborate.[5–7] The small premelting peaks on the heating process may be ascribed to the change in conformation of the alkyl chains.[22] Although detection of the liquid crystal to isotropic liquid transition was difficult for $C_8MIm(FH)_2F$ and $C_{10}MIm(FH)_2F$ by DSC, the results of POM and XRD indicated $C_{10}MIm(FH)_2F$ has a liquid crystalline mesophase with the clearing temperature of about 10 °C.

Figure 2 shows melting points and clearing temperatures of $C_xMIm(FH)_2F$ plotted as a function of x. The clearing temperature shows a larger dependence on the alkyl chain

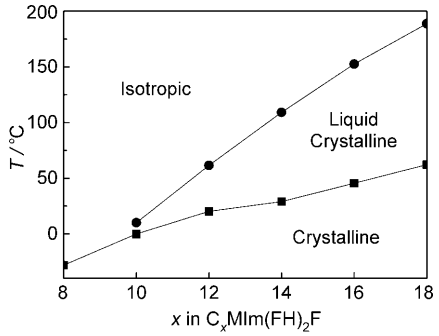

Figure 2. Melting points (■) and clearing temperatures (●) observed in the DSC thermogram (Table 1) of $C_xMIm(FH)_2F$ ($x=10$, 12, 14, 16, and 18).

length (from 10.0 to 188.8 °C) compared with the melting point (from −0.1 to 62.2 °C), leading to the wider temperature range of liquid crystalline mesophase for the cation with a longer alkyl chain (e.g., 10.1 °C for $C_{10}MIm(FH)_2F$ and 126.6 °C for $C_{18}MIm(FH)_2F$). This is mainly due to the increase in van der Waals interactions, as observed for other 1-alkyl-3-methylimidazolium ILCs with Cl^-, Br^-, BF_4^-, and PF_6^-.[4,6–7] The temperature range of the liquid crystalline mesophase follows the sequence $Cl^- > Br^- > (FH)_2F^- > BF_4^- > PF_6^- > OSO_2CF_3^-$, which can be explained by the ability of the anion to three-dimensionally form hydrogen bonds with an imidazolium-ring proton.[5] The $C_xMIm(FH)_2F$ salts ($x=14$, 16, and 18) show a relatively wide temperature range of liquid crystalline mesophase although it is not as wide as the chloride and bromide salts. The low melting point observed for ILCs based on $(FH)_2F^-$ arises from characteristics of the anion as is the case for ionic liquids based on $(FH)_nF^-$.[14]

Structural properties: Figure 3 shows a polarized optical microscopic (POM) texture of $C_{12}MIm(FH)_2F$, which is typical of the $C_xMIm(FH)_2F$ salts ($x=12$, 14, 16, and 18) and characterized by spontaneous formation of smooth fan-like or

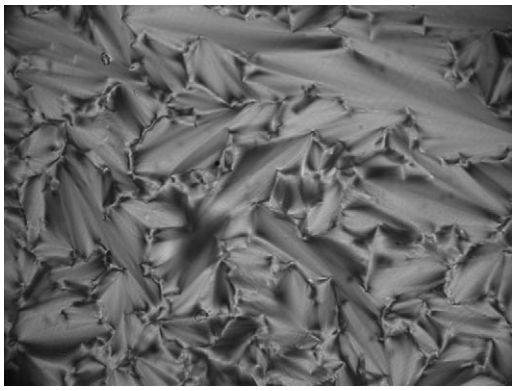

Figure 3. Polarized optical microscopic texture of $C_{12}MIm(FH)_2F$ at 50 °C.

focal conic textures. A similar texture was observed for $C_{10}MIm(FH)_2F$, but was much dimmer than the other cases, probably because of the weak alkyl–alkyl interaction for the shorter alkyl chain. The broken fan-like texture which is indicative of the smectic C mesophase was not observed for $C_{12}MIm(FH)_2F$ in the liquid crystalline mesophase on cooling from the isotropic phase to the crystalline phase, suggesting the absence of the smectic C mesophase in this system (Figure S3, Supporting Information).[23–24] These results of POM suggest that the liquid crystalline mesophase of $C_xMIm(FH)_2F$ is assigned to smectic A mesophase.[2,4,6–7] Such an enantiotropic smectic A liquid crystalline mesophase was also observed for other 1-alkyl-3-methylimidazolium ILCs in previous reports, since the cation dominates formation of the smectic layer.[4–7] These observations stand in contrast to ILCs based on pyrrolidinium, piperidinium, piperazinium, and morpholinium, which show a variety of textures because these ILCs exhibit various mesophases.[25] Confirmation of liquid crystal–isotropic liquid transition by POM was technically difficult for some cases ($x=14$, 16, and 18) because of the high levels of HF dissociation at their clearing temperatures.

Figure 4 shows the XRD patterns of the crystalline phase and liquid crystalline mesophase for $C_xMIm(FH)_2F$ ($x=10$, 12, 14, 16, and 18) in the low-angle region ($2° < 2\theta < 6°$) and Table 2 lists the layer spacings (d) for them (see Figure S4 and S5 in the Supporting Information for the XRD patterns of the crystalline phase and liquid crystalline mesophase, respectively, in the high-angle region, $5° < 2\theta < 30°$). Sharp peaks are observed in the low-angle region for both the crystalline phase and liquid crystalline mesophase, indicating formation of layered structures. No peak was found in the region lower than 2.0° in either case. The peaks of

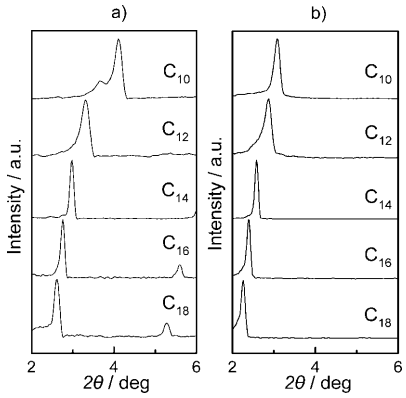

Figure 4. X-ray diffraction patterns for $C_xMIm(FH)_2F$ ($x=10$, 12, 14, 16, and 18) in a) crystalline phase (−60 °C for C10, −20 °C for C12 and C14, 10 °C for C16, and 50 °C for C18) and b) liquid crystalline mesophase (5 °C for C10, 30 °C for C12, 40 °C for C14, 50 °C for C16, and 65 °C for C18).

Table 2. Layer spacings (d) for $C_xMIm(FH)_2F$ ($x=10$, 12, 14, 16, and 18).

x	d in crystal [Å]	d in liquid crystal [Å]
10	21.7 at −60 °C	28.6 at 5 °C
12	26.6 at −20 °C	30.4 at 30 °C
14	29.6 at −20 °C	34.2 at 40 °C
16	32.0 at 10 °C	36.8 at 50 °C
18	33.7 at 50 °C	39.0 at 65 °C

$C_xMIm(FH)_2F$ ($x=14$, 16, and 18) are sharper than those of $C_xMIm(FH)_2F$ ($x=10$ and 12) in the liquid crystalline mesophase, indicating the more highly ordered structure of the cations with the longer alkyl chain. A small peak ascribed to the supercooled ILC was also observed at the low 2θ-angle side of the main peak in the case of $C_{10}MIm(FH)_2F$ ($2\theta=3.70°$). A similar phenomenon was also observed for $C_{12}MIm(FH)_2F$ when the cooling rate was fast. Absence of additional peaks in the higher 2θ-angle region ($6°<2\theta<30°$) suggests the loss of positional ordering within the layer plane (Figure S5, Supporting Information). To our knowledge, this is the first case of the ILC having the $C_{10}MIm^+$ cation.

Figure 5 shows layer spacings (d) of $C_xMIm(FH)_2F$ ($x=10$, 12, 14, 16, and 18) plotted against x. The layer spacing increases gradually against x in both the crystalline phase and liquid crystalline mesophase. The layer spacing d is found to satisfy $l<d<2l$, where l is the fully extended length of the cation and is roughly estimated from crystallographic data.[26] This result indicates an interdigitated bilayer structure is formed in the smectic A liquid crystalline mesophase (smectic A_2)[5] as shown in Figure 6. It is likely that the alkyl chain of the cation is tilted with respect to the layer plane in the crystalline phase,[5–6] since the smaller layer spacings are observed in the crystalline phase compared with the liquid crystalline mesophase. By taking previous data into account,[5] the layer spacing for smectic A_2 liquid crystalline mesophase of 1-alkyl-3-methylimidazolium

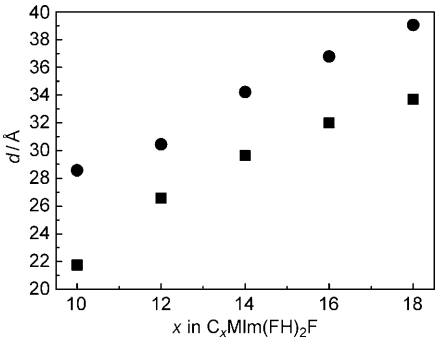

Figure 5. Layer spacings of $C_xMIm(FH)_2F$ ($x=10$, 12, 14, 16, and 18) in the crystalline phase (■) and liquid crystalline mesophase (●). See Figure 4 for the measurement temperature of each sample.

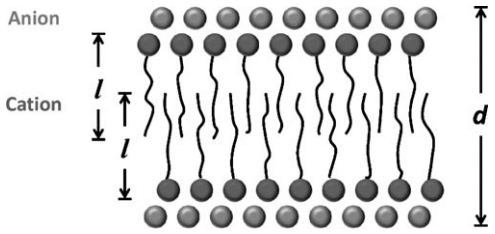

Figure 6. Schematic illustration of the interdigitated bilayer structure of the smectic A_2 liquid crystalline mesophase.

salts with various anions follows the sequence $Cl^->Br^->(FH)_2F^->BF_4^->OSO_2CF_3^-$. This is the same as the sequence of temperature range for the ILC mesophase and can be explained by the different anion–cation interactions within the polar region including hydrogen bonding.

Figure 7 shows XRD patterns of $C_{12}MIm(FH)_2F$ in the crystalline phase and liquid crystalline mesophase at different temperatures. Figure 8 shows the layer spacing against temperature for $C_{12}MIm(FH)_2F$ and Table 3 lists the layer spacing at each temperature. The shift of the main peak in the crystalline phase is negligible, whereas that in the liquid crystalline mesophase shifts to the high angle with an in-

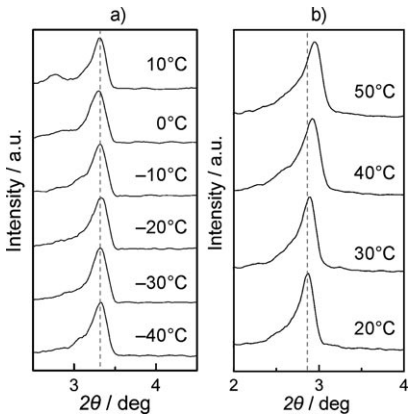

Figure 7. X-ray diffraction patterns in the low-angle region of a) crystalline phase and b) liquid crystalline mesophase for $C_{12}MIm(FH)_2F$ at different temperatures.

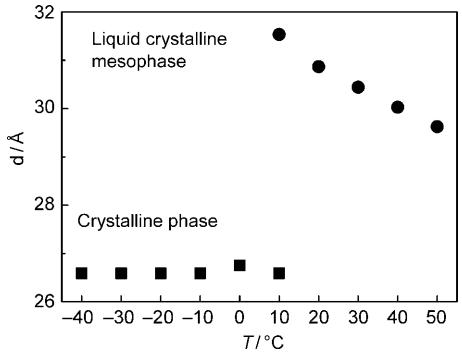

Figure 8. Layer spacings of $C_{12}MIm(FH)_2F$ in crystalline phase (■) and liquid crystalline mesophase (●) at different temperatures.

Table 3. Layer spacings (d) for $C_{12}MIm(FH)_2F$ at different temperatures.

T [°C]	d in crystal [Å]	d in liquid crystal [Å]
−40.0	26.6	–
−30.0	26.6	–
−20.0	26.6	–
−10.0	26.6	–
0.0	26.7	–
10.0	26.6	31.5
20.0	–	30.9
30.0	–	30.4
40.0	–	30.0
50.0	–	29.6

crease in temperature.[5] In the smectic C mesophase, the tilted angle of the layer structure decreases with increasing temperature, leading to an increase of the layer spacing (Figure S6, Supporting Information), whereas in the smectic A mesophase, the bilayer structure interdigitates more deeply with increasing temperature due to the increase of thermal mobility of the alkyl chains, leading to a decrease of the layer spacing. The observation for $C_{12}MIm(FH)_2F$ fits the latter case, which agrees with the results of POM.

Anisotropic ionic conductivity: Conductivity parallel ($\sigma_{\parallel}$) and perpendicular ($\sigma_{\perp}$) to the smectic layer was measured for $C_xMIm(FH)_2F$ ($x=10$, 12, 14, and 16). The cell using gold and ITO glass electrodes was used for this measurement (See Figures S7–S10 in the Supporting Information and references[8–11]). Since HF liberated from the fluorohydrogenate salts at elevated temperatures reacted with the glass substrate, $\sigma_{\parallel}$ and $\sigma_{\perp}$ could be measured up to 45 and 65 °C, respectively. Measurement of the conductivity of $C_{18}MIm(FH)_2F$ was difficult due to its relatively high melting point (62.2 °C). In contrast to the other ILCs reported previously, cooling down from the isotropic phase or shearing in the liquid crystalline mesophase[8–10] is not indispensable for the alignment of these fluorohydrogenate ILCs, probably due to their simple structures and relatively lower viscosity. Focal conic textures along with pseudo-isotropic domains were observed when the sample was placed in the conductivity measurement cell, whereas it turned into a totally pseudo-isotropic state when a pressure on the glass was applied (Figure S11, Supporting Information). Rotation of the sample on the stage did not change the vision, indicating formation of a homeotropic alignment.[24]

Figure 9 shows the temperature dependence of $\sigma_{\parallel}$ and $\sigma_{\perp}$ for $C_xMIm(FH)_2F$ ($x=10$, 12, 14, and 16) (See Table S2 in the Supporting Information for the $\sigma_{\parallel}$ and $\sigma_{\perp}$ values at each

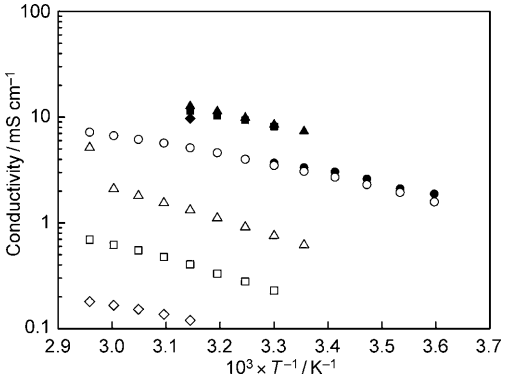

Figure 9. Temperature dependence of anisotropic ionic conductivity for $C_xMIm(FH)_2F$ ($\sigma_{\parallel}$: $x=10$ (●), 12 (▲), 14 (■), and 16 (◆); $\sigma_{\perp}$: $x=10$ (○), 12 (△), 14 (□), and 16 (◇)).

temperature). The $C_{10}MIm(FH)_2F$ salt does not exhibit significant anisotropy in ionic conductivity. This is probably because the decyl group is not long enough to form a highly ordered mesophase, although the POM somewhat showed formation of structural domains. For the $C_xMIm(FH)_2F$ salts ($x=12$, 14, and 16), $\sigma_{\parallel}$ is at least ten times higher than $\sigma_{\perp}$, suggesting the high ion mobility in the ionic layer as shown in Figure 6. The conductivity of ionic liquids based on 1-alkyl-3-methylimidazolium cation usually decreases with increasing alkyl chain length because of the increase in viscosity,[14] whereas $\sigma_{\parallel}$ for $C_xMIm(FH)_2F$ ($x=12$, 14, and 16) shows a higher conductivity than $C_{10}MIm(FH)_2F$ owing to formation of the well-ordered ion-conductive layers. The slight decrease in $\sigma_{\parallel}$ with increasing x from 12 to 16 may be explained by reduction of the number of ion-conductive layers per unit length if the mobility of the ionic species in the layer is the same in the three salts. As was suggested for the $I-I_3^-$ system in a smectic layer,[11] the dominant charge carrier in these ion-conductive layers is thought to be $(FH)_2F^-$, since the cation is much larger than the anion and linked to the adjacent cation by van der Waals interactions. Such a conduction mechanism implies application of the fluorohydrogenate ILCs as electrolytes in the electrochemical systems in which the fluorohydrogenate anion is involved with the electrode reactions. On the other hand, $\sigma_{\perp}$ shows a much sharper decrease with increasing alkyl chain length than $\sigma_{\parallel}$, leading to the increase in anisotropy of ionic conductivity from C_{12} to C_{16}. This observation indicates the insulating alkyl chain layers are developed more by introducing the longer alkyl chain. The discontinuous gap of $\sigma_{\perp}$ at the clearing temperature of $C_{12}MIm(FH)_2F$ (61.5 °C) results from the breakup of the layer structure. Temperature dependence of $\sigma_{\parallel}$ is similar to that of $\sigma_{\perp}$. Previous work on

the conductivity of some other ion-conductive liquid crystals also reported the same results.[8–11,27] Although the mechanisms of ion transport perpendicular to and parallel to the smectic layer are different to each other, these results suggest the activation energies are not.

Conclusion

The thermal, structural, and ion-conductive properties of 1-alkyl-3-methylimidazolium fluorohydrogenate ILCs, $C_xMIm(FH)_2F$ ($x=10$, 12, 14, 16, and 18), were investigated. The ILCs show a smectic A texture in the liquid crystalline mesophase and the temperature range of the mesophase increases with increasing alkyl chain length. The layer spacing of the interdigitated bilayer structures increases with increasing alkyl chain length both in the crystalline phase and liquid crystalline mesophase. The large anisotropy was observed in the ionic conductivity of $C_xMIm(FH)_2F$ ($x=12$, 14, and 16) because of formation of the smectic layer structure and the degree of the anisotropy increases with the increase in the alkyl chain length of the cation.

Experimental Section

General: Volatile materials were handled in a vacuum line constructed of SUS316 stainless steel and PFA (tetrafluoroethylene-perfluoroalkylvinylether copolymer). Nonvolatile materials were handled under a dry Ar atmosphere in a glove box. The starting chlorides, C_xMImCl ($x=8$, 10, 12, 14, 16, and 18), were prepared by reactions of 1-methylimidazole (Aldrich, 99%) and an equimolar quantity of the corresponding chloroalkanes (1-chlorooctane (Wako Chemicals, 95%), 1-chlorodecane (Wako Chemicals, 95%), 1-chlorododecane (TCI-EP, 97%), 1-chlorotetradecane (Aldrich, 98%), 1-chlorohexadecane (Wako Chemicals, 95%), 1-chlorooctadecane (Wako Chemicals, 95%)) at temperatures ranging from 70 to 100 °C for several days as described in the literature.[14] Purification of the chlorides was performed by dissolving the salts in acetonitrile (dehydrated, Wako Chemicals, 99%) and then precipitating from the solution by adding ethyl acetate (dehydrated, Wako Chemicals, 99.5%). Anhydrous HF (Daikin Industries) was dried over K_2NiF_6 prior to use. IR spectra of solid and liquid samples were obtained by use of an FTS-165 spectrometer (BIO-RAD Laboratories). The samples were sandwiched between a pair of AgCl crystal windows in an airtight cell made of stainless steel. Thermogravimetric and DSC analysis was performed under a dry Ar gas flow using Shimadzu DTG-60H and Shimadzu DSC-60, respectively, at the scanning rate of 5 °C min^{-1}. The sample was placed in a Ni open cell for TG and in a sealed cell made of stainless steel for DSC. Polarized optical microscopy was carried out using a VHX digital microscope (Keyence) under cross-polarized light at ×100 magnification. The sample was placed in a transparent cell made of sapphire and covered with a piece of glass substrate. The temperature was controlled by TS1500 hot stage unit (Japan High Tech). X-ray diffraction was performed using a Rigaku Ultima IV diffractometer ($Cu_{K\alpha}$, $\lambda=1.542$ Å). The output power was set as 40 kV-40 mA. The data were recorded in the 2θ ranges of 2–6° (scanning rate of 1° per minute) and of 2–30° (scanning rate of 2° per minute) with a step of 0.02°. The sample was sealed in a vacuum cell. The heating and cooling rate of 5 °C min^{-1} was used. The ionic conductivity was measured by impedance technique using PARSTAT 2273 electrochemical measurement system (Princeton Applied Research). Ionic conductivities, $\sigma_{\parallel}$ and $\sigma_{\perp}$, were measured according to the previously reported method.[8–10,27] A pair of comb-shaped gold electrodes were used to measure $\sigma_{\parallel}$ (Figure S7 and S8, Supporting Information). Gold (about 0.8 μm in thickness) was deposited on a borosilicate glass substrate in a comb shape after treatment of indium tin oxide (ITO) deposition (about 0.1 μm) in the same pattern to reinforce the contact on the glass. The sample was placed in the comb-shaped region covered with a piece of glass substrate to help the alignment. A pair of ITO (indium tin oxide) glass electrodes was used to measure $\sigma_{\perp}$ (Figure S9 and S10, Supporting Information).[8–10,27] The sample was sandwiched with two ITO glass electrodes and fixed with a Teflon spacer (50 μm in thickness). The cell constants of these cells were calibrated with a KCl aqueous solution (0.747 g kg^{-1}), $EMImBF_4$ (Kanto Kagaku) and $BMImPF_6$ (Kanto Kagaku). These conductivity measurement cells were placed in an airtight cell to avoid the effects of water (see Figure S12 in the Supporting Information for a schematic drawing of the airtight cell). The cell was held at each temperature for more than one hour to obtain a steady resistance and the measurement was repeated several times to confirm reproducibility of the data. No etching of the glass surface was observed after the mesurement.

Synthesis of $C_xMIm(FH)_2F$: The starting chloride, C_xMImCl, was weighed in a PFA reactor under a dry Ar atmosphere and a large excess of anhydrous HF was distilled on that at −196 °C. The mixture reacted on warming up to room temperature and the volatile gases were roughly eliminated by evacuation using a rotary pump. Elimination of the volatile gases and addition of fresh HF were repeated for effective elimination of chloride in the form of hydrogen chloride from the salt. Fluorohydrogenate salts $C_xMIm(FH)_nF$ with the specific HF composition of 2.0 were prepared by removing HF at elevated temperatures or mixing two fluorohydrogenate salts with different n values (less than and greater than 2.0). The HF composition of the obtained salts was confirmed by elemental analysis and titration using aqueous 0.1029 M NaOH (see Table S1 in the Supporting Information for the results of determination of the HF composition).

Acknowledgements

This work was financially supported by a Grant-in-Aid for Scientific Research from the Japan Society for the Promotion of Science, 20246140. The authors gratefully acknowledge the advice on conductivity measurement by Prof. Hiroyuki Ohno of Tokyo University of Agriculture and Technology.

[1] T. Welton, *Chem. Rev.* **1999**, *99*, 2071–2083.
[2] K. Binnemans, *Chem. Rev.* **2005**, *105*, 4148–4204.
[3] T. Kato, *Science* **2002**, *295*, 2414–2418.
[4] C. J. Bowlas, D. W. Bruce, K. R. Seddon, *Chem. Commun.* **1996**, 1625–1626.
[5] A. E. Bradley, C. Hardacre, J. D. Holbrey, S. Johnston, S. E. J. McMath, M. Nieuwenhuyzen, *Chem. Mater.* **2002**, *14*, 629–635.
[6] C. M. Gordon, J. D. Holbrey, A. R. Kennedy, K. R. Seddon, *J. Mater. Chem.* **1998**, *8*, 2627–2636.
[7] J. D. Holbrey, K. R. Seddon, *J. Chem. Soc. Dalton Trans.* **1999**, 2133–2139.
[8] a) M. Yoshio, T. Kagata, K. Hoshino, T. Mukai, H. Ohno, T. Kato, *J. Am. Chem. Soc.* **2006**, *128*, 5570–5577; b) M. Yoshio, T. Mukai, H. Ohno, T. Kato, *J. Am. Chem. Soc.* **2004**, *126*, 994–995.
[9] H. Shimura, M. Yoshio, K. Hoshino, T. Mukai, H. Ohno, T. Kato, *J. Am. Chem. Soc.* **2008**, *130*, 1759–1765.
[10] a) M. Yoshio, T. Mukai, K. Kanie, M. Yoshizawa, H. Ohno, T. Kato, *Adv. Mater.* **2002**, *14*, 351–354; b) T. Mukai, M. Yoshio, T. Kato, M. Yoshizawa, H. Ohno, *Chem. Commun.* **2005**, 1333–1335.
[11] N. Yamanaka, R. Kawano, W. Kubo, T. Kitamura, Y. Wada, M. Watanabe, S. Yanagida, *Chem. Commun.* **2005**, 740–742.
[12] R. Hagiwara, T. Hirashige, T. Tsuda, Y. Ito, *J. Fluorine Chem.* **1999**, *99*, 1–3.
[13] R. Hagiwara, T. Hirashige, T. Tsuda, Y. Ito, *J. Electrochem. Soc.* **2002**, *149*, D1–D6.

[14] R. Hagiwara, K. Matsumoto, Y. Nakamori, T. Tsuda, Y. Ito, H. Matsumoto, K. Momota, *J. Electrochem. Soc.* **2003**, *150*, D195–D199.
[15] a) K. Matsumoto, R. Hagiwara, Y. Ito, *Electrochem. Solid-State Lett.* **2004**, *7*, E41–E44; b) Y. Saito, K. Hirai, K. Matsumoto, R. Hagiwara, Y. Miyazaki, *J. Phys. Chem. B* **2005**, *109*, 2942–2948.
[16] a) S. Kanematsu, K. Matsumoto, R. Hagiwara, *Electrochem. Commun.* **2009**, *11*, 1312–1315; b) M. Yamagata, S. Konno, K. Matsumoto, R. Hagiwara, *Electrochem. Solid-State Lett.* **2009**, *12*, F9–F12.
[17] A. Senda, K. Matsumoto, T. Nohira, R. Hagiwara, *J. Power Sources* **2010**, *195*, 4414–4417.
[18] a) R. Hagiwara, T. Nohira, K. Matsumoto, Y. Tamba, *Electrochem. Solid-State Lett.* **2005**, *8*, A231–A233; b) J. Lee, T. Nohira, R. Hagiwara, *J. Power Sources* **2007**, *171*, 535–539.
[19] T. Fuchigami, *J. Fluorine Chem.* **2007**, *128*, 311–316.
[20] R. Hagiwara, Y. Nakamori, K. Matsumoto, Y. Ito, *J. Phys. Chem. B* **2005**, *109*, 5445–5449.
[21] a) J. H. Clark, J. Emsley, D. J. Jones, R. E. Overrill, *J. Chem. Soc. Dalton Trans.* **1981**, 1219–1222; b) T. V. Rosenvinge, M. Parrinello, M. L. Klein, *J. Chem. Phys.* **1997**, *107*, 8013–8019; c) W. D. Chandler, K. E. Johnson, J. L. E. Campbell, *Inorg. Chem.* **1995**, *34*, 4943–4949; d) I. Gennick, K. M. Harmon, M. M. Potvin, *Inorg. Chem.* **1977**, *16*, 2033–2040.
[22] K. Nishikawa, S. Wang, H. Katayanagi, S. Hayashi, H. Hamaguchi, Y. Koga, K. Tozaki, *J. Phys. Chem. B* **2007**, *111*, 4894–4900.
[23] K. Goossens, K. Lava, P. Nockemann, K. Van Hecke, L. Van Meervelt, P. Pattison, K. Binnemans, T. Cardinaels, *Langmuir* **2009**, *25*, 5881–5897.
[24] I. Dierking, *Textures of Liquid Crystals*, Wiley-VCH, Weinheim, **2003**.
[25] a) K. Goossens, K. Lava, P. Nockemann, K. Van Hecke, L. Van Meervelt, K. Driesen, C. Görller-Walrand, K. Binnemans, T. Cardinaels, *Chem. Eur. J.* **2009**, *15*, 656–674; b) K. Lava, K. Binnemans, T. Cardinaels, *J. Phys. Chem. B* **2009**, *113*, 9506–9511.
[26] a) Z. Wei, X. Wei, S. Fu, J. Liu, D. Zhang, *Acta Crystallogr. Sect. E* **2009**, *65*, o1159; b) A. Getsis, A.-V. Mudring, *Acta Crystallogr. Sect. E* **2005**, *61*, o2945–o2946; c) J. De Roche, C. M. Gordon, C. T. Imrie, M. D. Ingram, A. R. Kennedy, F. Lo Celso, A. Triolo, *Chem. Mater.* **2003**, *15*, 3089–3097; d) W. M. Reichert, J. D. Holbrey, R. P. Swatloski, K. E. Gutowski, A. E. Visser, M. Nieuwenhuyzen, K. R. Seddon, R. D. Rogers, *Cryst. Growth Des.* **2007**, *7*, 1106–1114; e) K. Goossens, P. Nockemann, K. Driesen, B. Goderis, C. Görller-Walrand, K. Van Hecke, L. Van Meervelt, E. Pouzet, K. Binnemans, T. Cardinaels, *Chem. Mater.* **2008**, *20*, 157–168.
[27] K. Kishimoto, T. Suzawa, T. Yokota, T. Mukai, H. Ohno, T. Kato, *J. Am. Chem. Soc.* **2005**, *127*, 15618–15623.

Received: May 19, 2010
Published online: September 30, 2010

